Smart Structures and Systems, *Vol. 24, No. 6 (2019) 769-781*
DOI: https://doi.org/10.12989/sss.2019.24.6.769

A vision-based system for long-distance remote monitoring of dynamic displacement: experimental verification on a supertall structure

Yi-Qing Ni*[1,2], You-Wu Wang[1,2a], Wei-Yang Liao[1b] and Wei-Huan Chen[3c]

[1]*Department of Civil and Environmental Engineering, The Hong Kong Polytechnic University, Hung Hom, Kowloon, Hong Kong*
[2]*Hong Kong Branch of Chinese National Rail Transit Electrification and Automation Engineering Technology Research Center, Hong Kong*
[3]*Department of Applied Mechanics and Engineering, Sun Yat-sen University, Guangzhou 510275, China*

(Received June 26, 2019, Revised August 20, 2019, Accepted August 29, 2019)

Abstract. Dynamic displacement response of civil structures is an important index for in-construction and in-service structural condition assessment. However, accurately measuring the displacement of large-scale civil structures such as high-rise buildings still remains as a challenging task. In order to cope with this problem, a vision-based system with the use of industrial digital camera and image processing has been developed for long-distance, remote, and real-time monitoring of dynamic displacement of supertall structures. Instead of acquiring image signals, the proposed system traces only the coordinates of the target points, therefore enabling real-time monitoring and display of displacement responses in a relatively high sampling rate. This study addresses the in-situ experimental verification of the developed vision-based system on the Canton Tower of 600 m high. To facilitate the verification, a GPS system is used to calibrate/verify the structural displacement responses measured by the vision-based system. Meanwhile, an accelerometer deployed in the vicinity of the target point also provides frequency-domain information for comparison. Special attention has been given on understanding the influence of the surrounding light on the monitoring results. For this purpose, the experimental tests are conducted in daytime and nighttime through placing the vision-based system outside the tower (in a brilliant environment) and inside the tower (in a dark environment), respectively. The results indicate that the displacement response time histories monitored by the vision-based system not only match well with those acquired by the GPS receiver, but also have higher fidelity and are less noise-corrupted. In addition, the low-order modal frequencies of the building identified with use of the data obtained from the vision-based system are all in good agreement with those obtained from the accelerometer, the GPS receiver and an elaborate finite element model. Especially, the vision-based system placed at the bottom of the enclosed elevator shaft offers better monitoring data compared with the system placed outside the tower. Based on a wavelet filtering technique, the displacement response time histories obtained by the vision-based system are easily decomposed into two parts: a quasi-static ingredient primarily resulting from temperature variation and a dynamic component mainly caused by fluctuating wind load.

Keywords: structural health monitoring; supertall structure; displacement measurement; vision-based system; real-time; long-distance; remote sensing

1. Introduction

Recent years have witnessed the growth of supertall structures built or being built in a number of densely urbanized cites worldwide. Examples are the Burj Khalifa of 828 m high in Dubai, United Arab Emirates; the Abraj AI-Bait Clock Tower of 601 m high in Saudi Arabia; the Lotte World Tower of 554.5 m high in South Korea; the One World Trade Center of 541.3 m high in United States. In China, more than ten skyscrapers over 500 m in height (the Shanghai Tower of 632 m high; the Canton Tower of 600 m high; the Pingan Finance Center of 599 m high; the Goldin Finance 117 of 597 m high; the Guangzhou CTF Finance Center of 530 m high; the Tianjin CTF Finance Center of 530 m high; and the China Zun of 528 m high among others) have been built. These complex skyscrapers are prone to temperature-induced quasi-static deformation and wind-induced vibrations. As a result, regular or continuous monitoring of the static and dynamic displacement of the structures during in-service stage is essential to detect anomalies in loading and response, and subsequently to assess/evaluate the structural integrity, safety, serviceability, and reliability. However, accurate measurement of structural displacement for high-rise buildings is still a challenging task.

Considerable research efforts have been devoted to the development of displacement measurement techniques which are mainly referred to contact transducers and non-contact sensors. For the contact transducers, the linear variable differential transformers (LVDTs) have been widely used for structural displacement measurement. This kind of sensors, however, needs a stationary reference

*Corresponding author, Chair Professor
E-mail: ceyqni@polyu.edu.hk
[a] Ph.D., Postdoctoral Fellow
[b] Ph.D., Research Associate
[c] Ph.D., Postdoctoral Fellow

ISSN: 1738-1584 (Print), 1738-1991 (Online)

platform. For large-scale civil engineering structures, such a stationary platform is in general not available for absolute displacement and deflection measurement. Alternatively, extensive studies have been conducted on indirect dynamic displacement measurement through double integration of the acquired acceleration data, while numerical errors resulting from this approach are inevitable and will accumulate with the evolution of time. As one category of non-contact sensors, global positioning system (GPS) has been widely applied for displacement measurement of high-rise structures (Lovse *et al*. 1995, Çelebi 2000, Breuer *et al*. 2002, Tamura *et al*. 2002, Ogaja *et al*. 2003, Brownjohn *et al*. 2004, Kijewski-Correa *et al*. 2006, Li *et al*. 2006, Seco *et al*. 2007, Ni *et al*. 2009). However, the measurement instruments are quite expensive, especially when the structural displacements at a large number of locations are desired to be synchronously measured. Another typical non-contact displacement measurement technique is laser Doppler vibrometer (LDV), which is capable of providing accurate multiple-location displacement measurement in certain distance; yet the devices are also costly and the laser intensity may become dangerously strong in some occasions (Nassif *et al*. 2005, Gordon and Lichti 2007, Park *et al*. 2007, Siringoringo and Fujino 2009).

With the rapid development of photonics and image processing technology, vison-based monitoring systems have attracted increasing attention and are becoming an effective alternative for structural displacement measurement. The research and applications of vison-based structural displacement measurement systems have been reported in the past two decades. Olaszek (1999) developed a method for investigating dynamic characteristics of bridges based on the photogram-metric principle using an additional reference system. A reference point concurrently measured with the target point was used to exclude the effect of translational movement at image capturing camera. The accuracy of the system was 0.11 mm at 10 m / 5 Hz and 1.15 mm at 100 m / 5 Hz. Wahbeh *et al.* (2003) employed a vison-based system to measure the bridge deck displacements of the Vincent Thomas Bridge (located in California, whose main span is about 457 m). Lee *et al.* (2007) and Fukuda *et al.* (2010) developed a real-time displacement measurement system using digital image processing techniques, which is highly cost-effective and easy to implement. The performance of the proposed system was verified through a shaking table test and a field test on a bridge with open-box girders. In the field test, a single target was located about 70 m in front of the camera. In order to measure displacements of multiple points at the same time, the investigators further developed a time synchronization system where TCP/IP protocol was employed for communications. Ji and Chang (2008) developed a new non-target technique based on image analysis using one digital camera for cable vibration measurement. To verify the proposed technique, a lab test on a rigid pipe sitting on a shake table and a field test on free vibration of a small pedestrian bridge cable were carried out. Chan *et al*. (2009) proposed a method using a charge-coupled-device (CCD) camera for vertical displacement measurements of bridges. This CCD camera method uses image processing techniques for pixel identification and subsequent edge detection. Laboratory tests were carried out to validate the efficiency and precision of the proposed method. Recently, Ye *et al*. (2013, 2015a, b, 2016a, b, c, 2017) have conducted a series of research work on vision-based structural displacement measurement of long-span bridges, mainly focusing on algorithm development, laboratory tests and field applications.

While considerable work has been carried on structural displacement measurement using vision-based techniques, development of a non-contact, cost-effective, real-time, long-distance and high-precision vision-based system for displacement measurement of high-rise buildings is still in high demand in that: (i) the current systems are confined to measure the dynamic displacement responses of structures with a measurement distance (distance between the target and the vision system) ranging in dozens of meters. For supertall structures, however, it is usually required to monitor the target located at a distance from the vision system ranging between several hundreds of meters and even over one thousand meters; (ii) for supertall structures, dynamic displacement under normal wind loading is of small magnitude, usually several centimeters, which requires higher accuracy and resolution of the system.

In order to cope with this problem, a system based on industrial digital camera and image processing has been developed for long-distance, remote, and real-time monitoring of static and dynamic displacement of supertall structures. The performance of the developed system is verified through field measurements of the top displacement of the Canton Tower of 600 m high at different operating conditions. Meanwhile, the achieved results, including structural displacement responses and modal frequencies, are compared with those obtained from GPS, accelerometer and finite element analysis.

2. Vision-based system for displacement measurement

2.1 System configuration

As illustrated in Fig. 1, the vision-based displacement measurement system comprises an industrial digital camera, an extend zoom lens, a laptop (or desk) computer, a Giga LAN wire, and tailor-made software. In this system, a long-distance image acquisition device is developed by integrating the Prosilica GigE GC2450 camera (its specifications are listed in Table 1) with the Navitar 24X zoom extender lens, which is capable of real-time tracking the target from a distance over one thousand meters with pattern matching techniques. In the field measurement of structural displacement, an LED light is usually fixed on the structure as the target to enable the measurement in night or bad weather as well when the structure is accessible; otherwise a remarkable point of the structure will be specified as an alternative target.

The measurement resolution of the system depends on the selection of camera, the target's movement range, and

the working (measurement) distance. In this study, the Prosilica GigE camera GC2450 is finally selected due to its high pixel resolution and acceptable price. The resolution (pixel) of the selected digital camera is 2456 pixels (horizontal) × 2058 pixels (vertical) with the sampling rate 15 frames per second. If the vertical movement range of the target is 400 mm with a measurement distance of 100 m away from the camera, the measurement accuracy is 400/2058 = 0.194 mm/pixel in vertical direction; while the measurement distance increased to 200 m away from the camera, the measurement accuracy becomes 2×400/2058 =0.389 mm/pixel.

The devised vision-based monitoring system for dynamic displacement measurement of supertall structures is illustrated in Fig. 2. In-situ calibration can be easily made when the distance of any two points in the vicinity of the target is known or by placing a ruler on the target location or a rigid bar attached with two LED lights in a fixed (known) distance. In the present study, the third approach was adopted to calibrate the movement of the target. At the beginning of experiment, two LED lights were lit for the displacement calibration. After that, one light was left on as target for subsequent long-term monitoring. A schematic view of these lights is shown in Fig. 3.

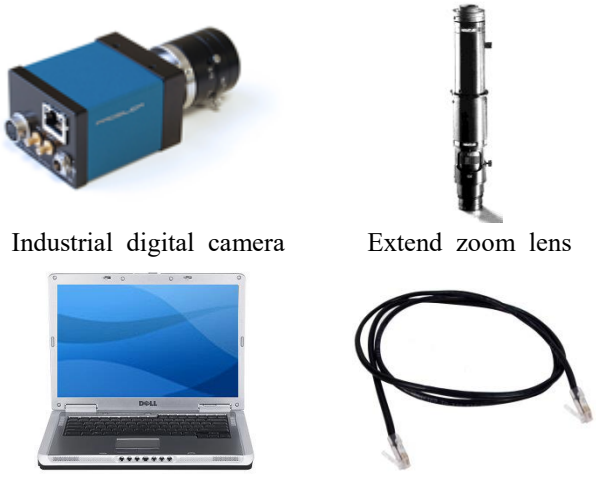

(a) Hardware

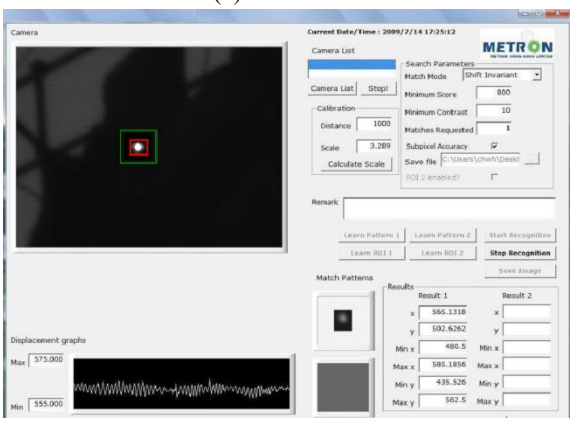

(b) Software

Fig. 1 Vision system configuration

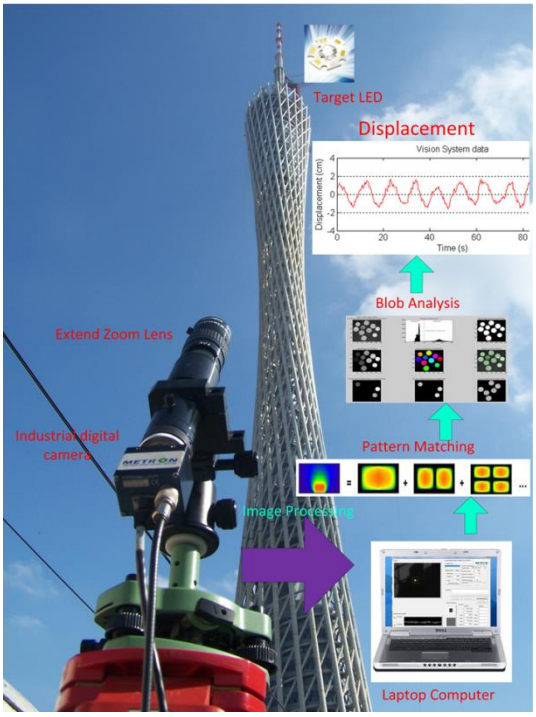

Fig. 2 Schematic of vision-based dynamic displacement measurement system

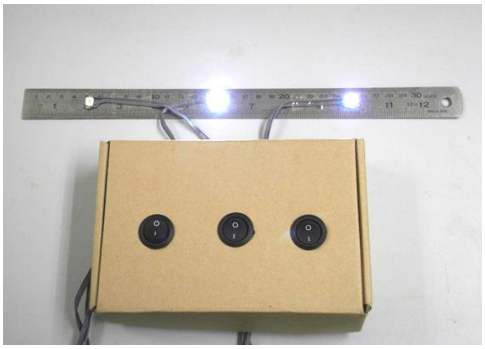

Fig. 3 High brightness LED target

Table 1 Camera model and parameters

Model No.	GC2450
CCD (inch)	2/3"
Frame rate (fps) / sampling frequency (Hz)	15
Camera resolution (pixel)	2456×2058
Connection cable	Giga Lan

The testing procedures are as follows:

- Aim at the target and tune the focus of lens until the target is clear;
- Light up 2 LED lights with known distance and draw a line between the two light sources by mouse in the computer screen. After inputting the known distance into scale field and clicking Calibration

Scale, the software will automatically calculate the distance (mm) per pixel according to the scale (Fig. 4(a));

- Leave one LED light burning as measurement target and draw a rectangle box covering the LED light by mouse, then click Learn Pattern to tell the software which target needs to be traced (Fig. 4(b));
- Draw a rectangle box covering the target allowable moving area and click Learn ROI (region of interest) to specify the measurement range (Fig. 4(c));

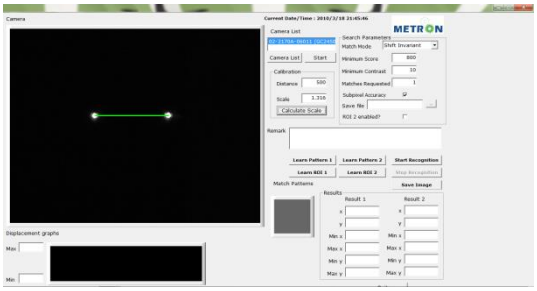

(a) In-situ calibration

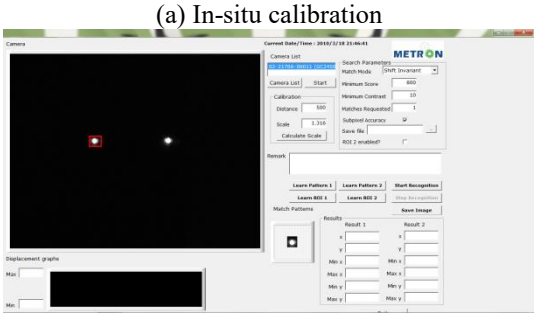

(b) Specifying the target

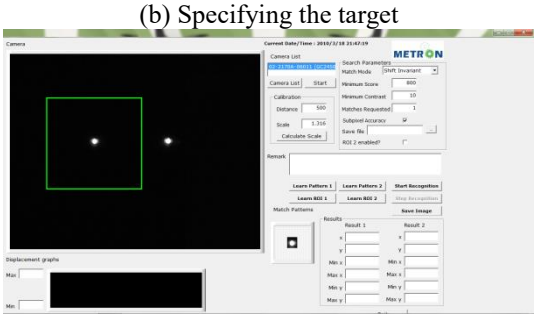

(c) Specifying the ROI

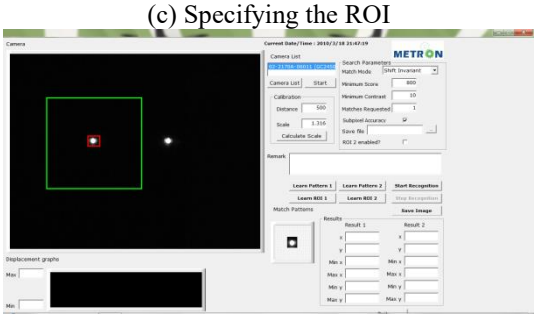

(d) Starting image processing

Fig. 4 Testing procedure of the system

- Click Start Recognition to start real-time recording the target coordinates (Fig. 4(d)). The structural displacement time series is derived from the obtained coordinates and the scale ratio between the actual size of the pattern and pixels of the pattern in image. During the acquisition of displacement, only the target coordinates rather than the image signals need to be stored in the computer, thus greatly reducing the computer deposit.

2.2 Image processing techniques

Pattern matching is an effective method for digital image processing, which is able to locate the target in an image that matches a predefined pattern (also referred to as a template) (Ye *et al*. 2013). The process involves two phases: an off-line learning phase in which the pattern is processed, and a matching phase that can be executed in real time.

The normalized cross-correlation is one of the most popular pattern matching algorithms. As shown in Fig. 5, the correlation $C(i, j)$ is defined as

$$C(i,j)=\sum_{x=0}^{l-1}\sum_{y=0}^{k-1} w(x,y)f(x+i,y+j) \tag{1}$$

where $w(x,y)$ is a pattern (template) of size $k\times l$, $f(x,y)$ is the original image of size $m\times n$ (where $k\le m$, $l\le n$); $i=0,1,\cdots m-1$, $j=0,1,\cdots n-1$.

Correlation computation is a process of moving the pattern $w(x,y)$ within the image area $f(x,y)$ and calculating the value $C(i, j)$ in that area, which involves the sum of multiplying each pixel in the pattern by the image pixel that it overlaps. The maximum value of $C(i, j)$ indicates the position (x,y) where the pattern $w(x,y)$ best matches the image $f(x,y)$. However, the correlation function in Eq. (1) has the disadvantage of being sensitive to scale changes of the pattern $w(x,y)$ and the image $f(x,y)$.

To overcome this problem, the normalized correlation coefficient is used to perform pattern matching, which is defined as

$$R(i,j)=\frac{\sum_{x=0}^{l-1}\sum_{y=0}^{k-1}(w(x,y)-w_{mean})(f(x+i,y+j)-f_{mean}(i,j))}{\sqrt{\sum_{x=0}^{l-1}\sum_{y=0}^{k-1}(w(x,y)-w_{mean})^2}\sqrt{\sum_{x=0}^{l-1}\sum_{y=0}^{k-1}(f(x+i,y+j)-f_{mean}(i,j))^2}} \tag{2}$$

where w_{mean} is the average value of the pixels in the pattern $w(x,y)$; and $f_{mean}(i,j)$ is the average value of the image area $f(x,y)$. It is known from Eq. (2) that the normalized correlation coefficient R has the values in the range [-1, 1], which is independent of scale changes of the pattern $w(x,y)$ and the image $f(x,y)$.

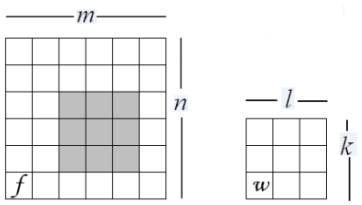

Fig. 5 Cross-correlation between predesigned pattern and captured image

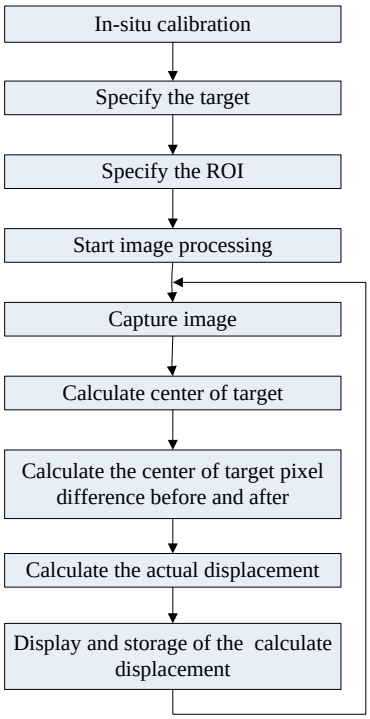

Fig. 6 Flowchart of vision-based structural displacement measurement

Fig. 6 shows the schematic flowchart of structural displacement measurement based on image processing techniques. It involves target calibration algorithms, projection of the captured image, actual displacement calculation using scaling factor and the number of pixels moved, display and storage of the calculated displacement. The quantity of information in need to be processed in real-time depends on the number of pixels per frame and the number of frames per second. Because the region of interest (ROI) (as shown in Fig. 4(c)) for target movement does not cover the whole image frame, the image processing is performed only within this confined region, minimizing the computational time in image processing. The entire software is implemented by using VB language.

Fig. 7 The Canton Tower

3. Monitoring of Canton Tower

3.1 The Canton Tower

The Canton Tower located in the city of Guangzhou, China, is a supertall structure with a height of 600 m (Fig. 7). It serves for sightseeing, office, catering, and entertainment including Ferris wheel, ceremony hall, observatory decks, 4D cinemas, revolving restaurants, open-air skywalk, etc. The Canton Tower comprises a main tower of 454 m high and an antennary mast of 146 m high founded on the top of the main tower. The main tower is composed of a reinforced concrete inner structure with an ellipse cross-section and a steel lattice outer structure with its cross-section in a form of hyperboloid generated by the rotation of two ellipses. The antennary mast is a steel spatial structure with an octagonal cross-section. A sophisticated long-term structural health monitoring (SHM) system has been implemented on the Canton Tower in synchronism with its construction to real time monitor the structural performance and safety at both in-construction and in-service stages (Ni *et al*. 2009, 2011, 2017, Xia *et al*. 2011). As the long-term SHM system consists of about 800 sensors including a GPS and over 20 accelerometers, when the vision-based system is implemented for dynamic displacement measurement of the Canton Tower, it is easy to acquire GPS and acceleration data concurrently for comparison and verification.

3.2 Scenario 1: monitoring outside the structure in daytime

The Canton Tower is an ideal testbed to verify the performance of the vision-based system for high-rise building displacement measurement, through comparing the

Fig. 8 The vision-based system located near the site office

measurement data obtained by the vision-based system and those acquired by the SHM system.

As shown in Fig. 8, the displacement measurement was first conducted in daytime when the main tower crane was working. The vision monitoring system was positioned at the ground near the site office, and the target point was located at the top of the main tower at a height of 454 m. To facilitate the comparison with the displacement responses obtained by GPS, the selected target point was placed in the vicinity of a GPS receiver (Fig. 9). As the Canton Tower is a typical supertall structure having first dozen modal frequencies within 2 Hz, the sampling frequencies of the vision-based system and GPS were both set as 5 Hz. The calibration was conducted in-situ by placing a rigid bar attached with two LED lights in a fixed distance. The lens was adjusted to the target and the coordinate of target was measured by a total station. The distance between the target on the tower and the vision-based system placed near the site office was about 523.2 m. The target allowable movement range was set as 400 mm, so the measurement accuracy was 5.232×400/2058 = 1.017 mm/pixel according to the calculation procedure provided in Section 2.1.

The tests were carried out in two days under different weather conditions. One was cloudy while the other was sunny. The GPS is capable of simultaneously measuring the dynamic displacement responses in three directions. Hence, the displacement components measured by the GPS are projected onto the same horizontal direction as the vision-based system for comparison.

The first test was conducted in cloudy daytime. Fig. 10 illustrates the horizontal displacement responses of the Canton Tower at the top of the main tower measured by the GPS. It is seen that there are many spikes and abnormal shifts before data correcting, which are due to specific positioning of the satellites and electro-magnetic interference in the construction site (top of the main tower). Fig. 11 shows a comparison of the horizontal displacement responses measured by the vision-based system (blue line) and GPS (red line). It is observed that the displacement responses measured by the vision-based system agree well with the corrected displacement measured by the GPS in time domain, but do not exhibit spikes and abnormal shifts. Therefore, the displacement responses measured by the vision-based system can directly be used to verify and correct the data measured by GPS.

The second test was conducted in sunshine daytime. Figs. 12 and 13 show a comparison of the horizontal displacement responses measured by the vison-based system (red line) and GPS (blue line), respectively. The horizontal displacement responses measured by the GPS in Fig. 12 are not corrected, while those in Fig. 13(a) are corrected. It can be observed that there are also many spikes and abnormal shifts in the displacement responses measured by the GPS before data correction. The displacement responses measured by the vision-based system agree better with the displacement responses measured by the GPS after data correction. Fig. 13(b) shows 100-second time histories of displacement responses measured by the vision-based system and GPS for more careful comparison. A vibration period of about 10 seconds is clearly observed.

Spectral analysis is conducted for the measured data from the vision-based system, GPS, and accelerometer (Fig. 14). The identified modal frequencies have also been compared with the predicted modal frequencies from a 3D finite element model (FEM) of the Canton Tower (Ni *et al.* 2012). As shown in Table 2, the fundamental modal frequencies obtained by the vision-based system, GPS, accelerometer, and finite element analysis are in a good agreement. The first mode is the bending vibration along the short-axis of the main tower.

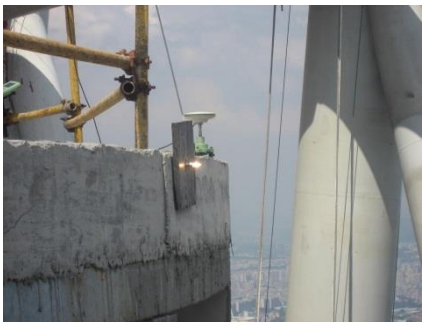

Fig. 9 Location of LED light and GPS receiver

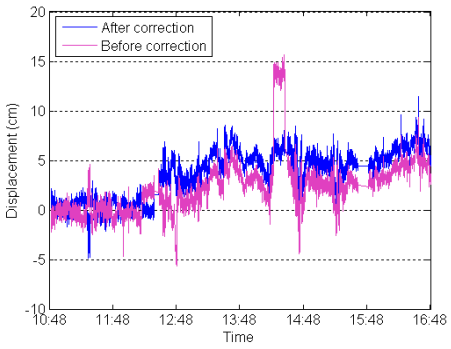

Fig. 10 GPS data before and after correction

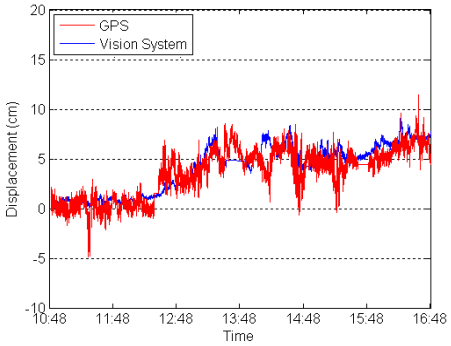

Fig. 11 Comparison of displacement responses measured by the vison-based system and GPS in cloudy daytime (GPS data after correction)

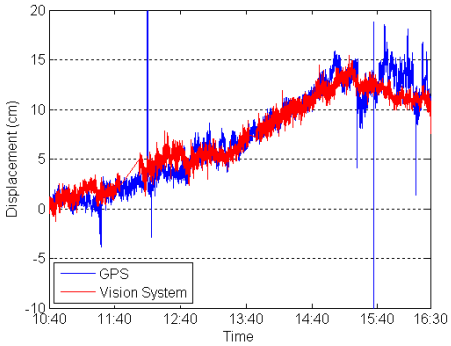

Fig. 12 Comparison of displacement responses measured by the vison-based system and GPS in sunshine daytime (GPS data before correction)

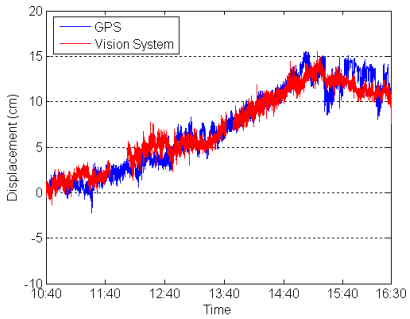

(a) Complete monitoring displacement responses

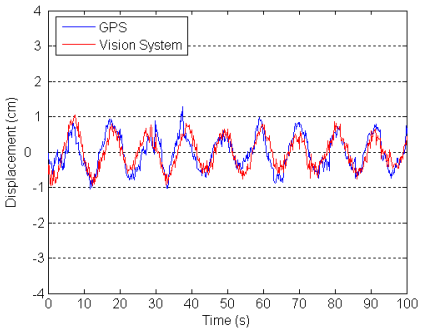

(b) Selected 100-second displacement responses

Fig. 13 Comparison of displacement responses measured by the vison-based system and GPS in sunshine daytime (GPS data after correction)

Table 2 Modal frequencies obtained in Scenario 1 (Hz)

Mode No.	Vision-based system	GPS	Accelerometer	FEM
Mode 1	0.0952	0.0952	0.0954	0.0995

3.3 Scenario 2: monitoring inside the structure at night

To eliminate the effects of the solar radiation and construction activities in daytime to the vision-based monitoring, the tests were carried out later in the elevator shaft of the main tower in the evening.

As shown in Fig. 15, both the vision-based system and target were placed in the elevator shaft, at the heights of 7.2 m and 448.8 m respectively. The target was set parallel to the short-axis direction of the inner structure (as shown in Fig. 16). The distance between the target and the vision-based system was about 440 m. As the target allowable movement range was also set as 400 mm, the measurement accuracy was 4.4×400/2058=0.855 mm/pixel. Meanwhile, GPS was installed for displacement response measurement, providing a way to compare with the results measured by the vision-based system.

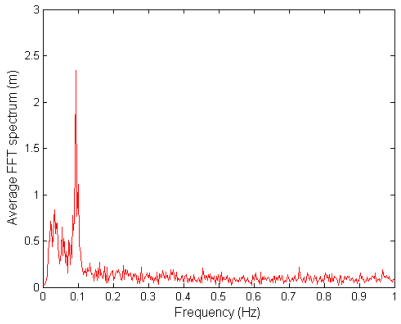

(a) Vision-based system

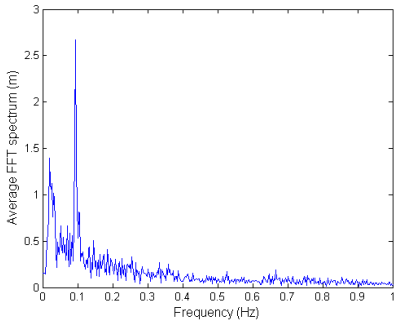

(b) GPS

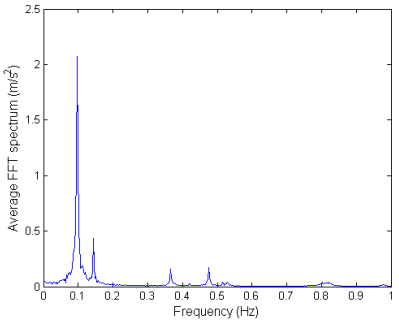

(c) Accelerometer

Fig. 14 Power spectra of the displacement/acceleration responses measured by the vision-based system, GPS, and accelerometer

Table 3 Modal frequencies obtained in Scenario 2 (Hz)

Mode No.	Vision-based system	GPS	Accelerometer	FEM
Mode 1	0.0946	0.0946	0.0944	0.0995
Mode 2	0.1369	0.1369	0.1367	0.1437

The GPS reference station was placed on the ground and the GPS receiver was set at the height of 459.2 m of the tower to meet the intervisibility requirement. Due to the complexity of the construction site, there was no suitable place close to the target for installing the GPS receiver and finally an open position at the height of 459.2 m was selected, which will cause the displacement responses measured by the GPS slightly larger than those measured by the vision-based system. The sampling rate was set as 5 Hz again for both the vision-based system and GPS. What's more, the wind and temperature monitored by the SHM system were used to evaluate the environmental impacts on the displacement responses.

First of all, the data measured by the GPS are projected onto the two measurement directions of the vision-based system. Fig. 17 shows a compassion of displacement responses measured by the vison-based system and GPS in two horizontal directions. It is observed that the displacement responses measured by the vision-based system agree fairly well with those measured by the GPS in time domain, but the amplitudes of displacement responses measured by the GPS are larger than those measured by the vision-based system. This is because the position of the GPS receiver is higher than the target.

Fig. 18 shows the power spectra of the displacement responses measured by the vison-based system and GPS, and the acceleration response measured by accelerometer at two horizontal directions. It is seen that the first two modal frequencies of the structure are accurately identified from the peaks of the spectra. As shown in Table 3, the first two modal frequencies obtained from the vison-based system, GPS, and accelerometer are in a good agreement. The first two modes are the structural bending vibration along its short-axis and long-axis, respectively. The first modal frequency obtained from Scenario 2 conducted at night is smaller than that obtained from Scenario 1 conducted in daytime. Environmental changes such as temperature variation probably explain the slight difference of the first modal frequency measured.

A wavelet multi-resolution analysis is further conducted for decomposition of the displacement responses obtained by the vision-based system and GPS. The results are shown in Fig. 19. As the average wind was steady during the test period, the high frequency (higher than 0.01 Hz) components could be regarded as the structural random vibration caused by wind loading while the low frequency (lower than 0.01 Hz) components correspond to the static displacement responses generated by temperature variation. It is observed from Fig. 19(a) and Fig. 20(a) that the variation tendency of the low-frequency components of the displacement responses is consistent with atmospheric temperature. So the low-frequency components of the displacement responses are mainly caused by temperature variation. It is believed that the displacement responses after eliminating the low-frequency components, as shown in Fig. 19(b), are mainly attributed to wind loading. The separation of quasi-static and dynamic response components is helpful to structural health monitoring.

3.4 Error evaluation

The normalized root mean square error (NRMSE) is used to evaluate the error between the displacement responses measured by the vision-based system and GPS. It is obtained by

$$NRMSE = \sqrt{\frac{\frac{1}{n}\sum_{i=1}^{n}(M_i - V_i)^2}{\frac{1}{n}\sum_{i=1}^{n}M_i^2}} = \sqrt{\frac{\sum_{i=1}^{n}(M_i - V_i)^2}{\sum_{i=1}^{n}M_i^2}} \quad (3)$$

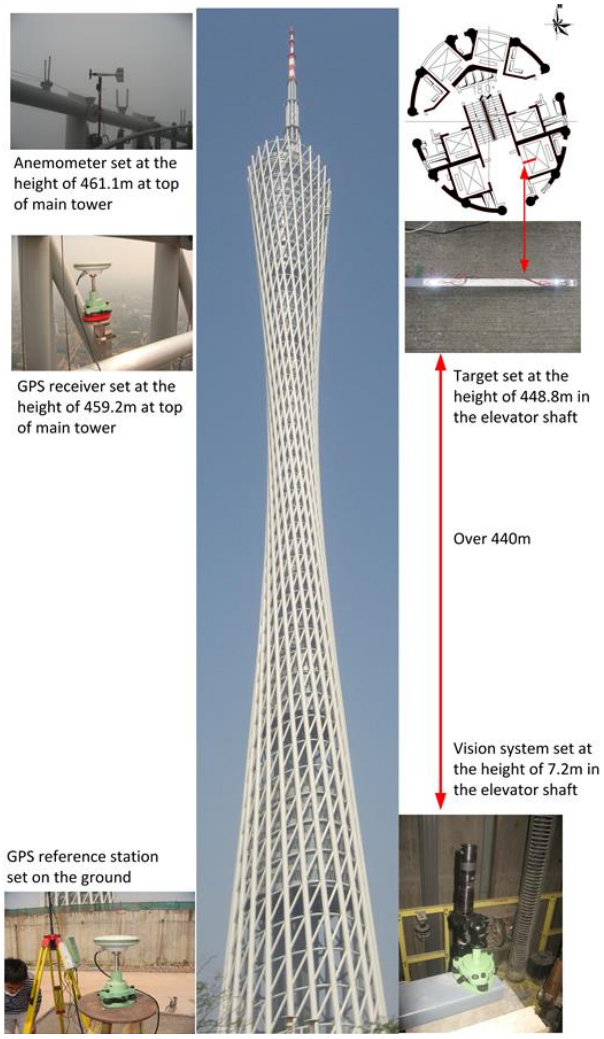

Fig. 15 The vision-based system positioned in the elevator shaft of the main tower

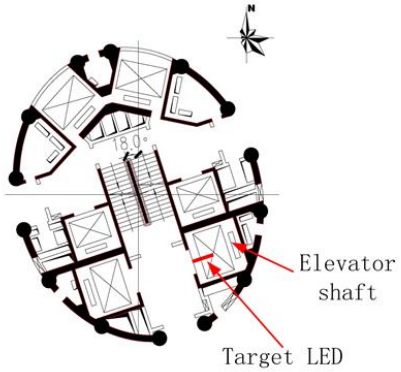

Fig. 16 Layout of target LED and elevator shaft

where M_i is the measured displacement by GPS; V_i is the measured displacement by the vision-based system; and n is the data number. The smaller the value of NRMSE, the smaller the relative error between M_i and V_i.

Table 4 lists the obtained error statistics. The values of NRMSE obtained under different cases show that the test conducted in the elevator shaft at night without site construction performs best. An adverse impact is brought out by the site construction on GPS and the changes of rays of light on the vision-based system.

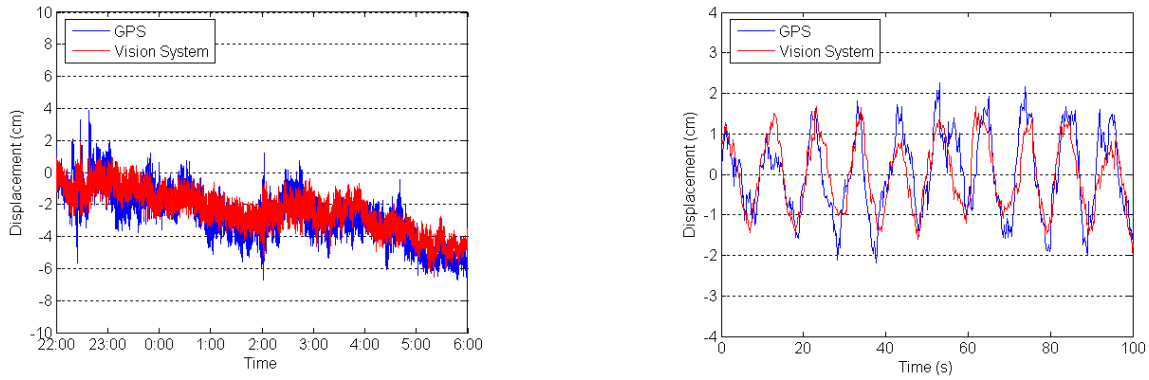

(a) Displacement responses in short-axis direction of inner structure

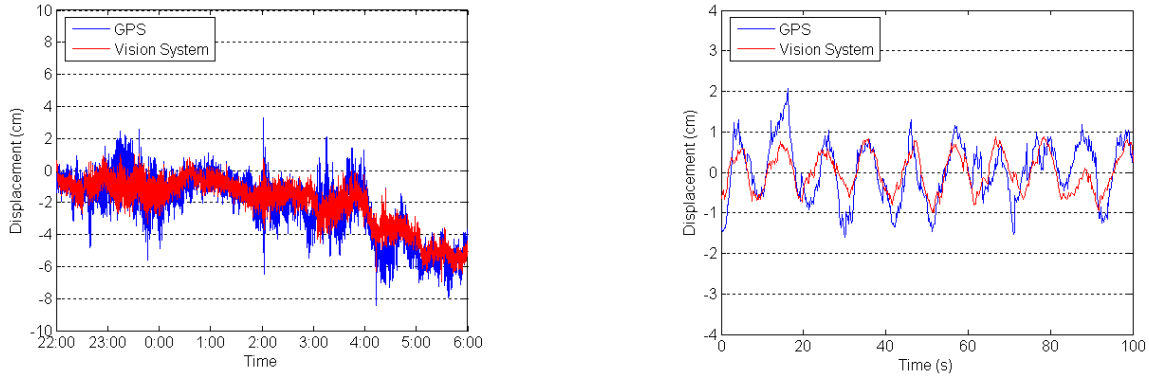

(b) Displacement responses in long-axis direction of inner structure

Fig. 17 Comparison of displacement responses measured by the vision-based system and GPS at night

Table 4 NRMSE obtained under different cases

No.	Environment	Construction	Location	NRMSE (%)
1	Cloudy, daytime	Y	Near the site office	35.0
2	Sunshine, daytime	Y	Near the site office	23.8
3	Cloudless, night	N	In the elevator shaft of the main tower	17.3

4. Conclusions

A vision-based system consisting of an industrial digital camera, an extend zoom lenses, a laptop (or desk) computer, and tailor-made software has been developed for long-distance, remote, and real-time monitoring of static and dynamic displacement responses of supertall structures. The developed image acquisition device is capable of capturing the digital images of a target on the structure over one thousand meters away. The structural displacement responses were derived in real-time through cross-correlation analysis between the predefined pattern and the captured digital images with the aid of a pattern matching algorithm. The performance of the developed vision-based system was evaluated by the field experiments of measuring the main tower displacement responses of the Canton Tower in different scenarios. Meanwhile, GPS and accelerometer were used together to measure the structural displacement responses and dynamic characteristics. The results indicate that the displacement responses measured by the vision-based system match well with those obtained by the GPS in time domain, but are less noise-corrupted. In frequency domain, the identified modal frequencies using the data measured from the vision-based system, GPS, and accelerometer are favorably consistent. Moreover, the impact of site construction and the changes of rays of light on the system performance have also been studied. It is shown that an adverse impact is brought out by the site construction on the GPS and the changes of rays of light on the vision-based system. Based on the field test results, it is concluded that the developed vision-based system enables non-contact, long-distance, and high-precision structural displacement response measurement for high-rise buildings. This system is also applicable to other large-scale civil structures such as long-span bridges, especially when contact-type displacement measurement becomes impossible or extremely difficult.

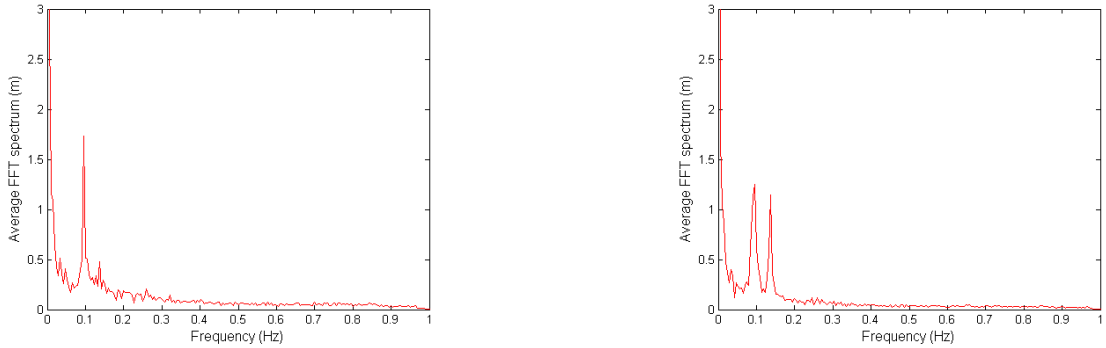

(a) Vision-based system: left – in short-axis direction; right – in long-axis direction

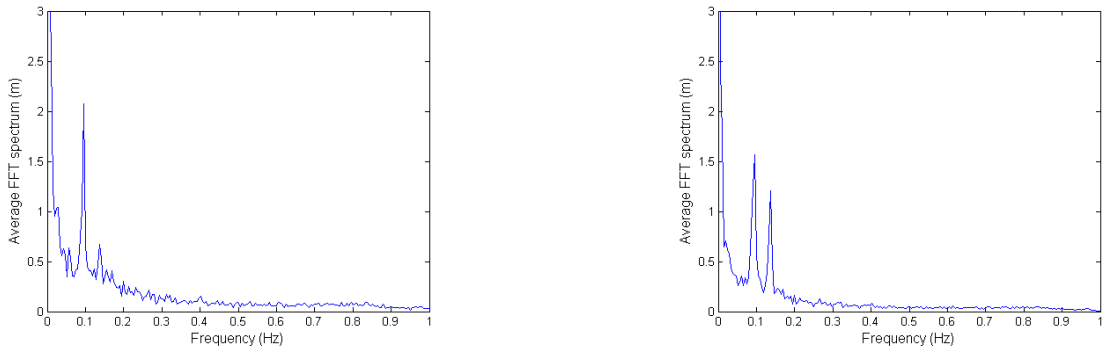

(b) GPS: left – in short-axis direction; right – in long-axis direction

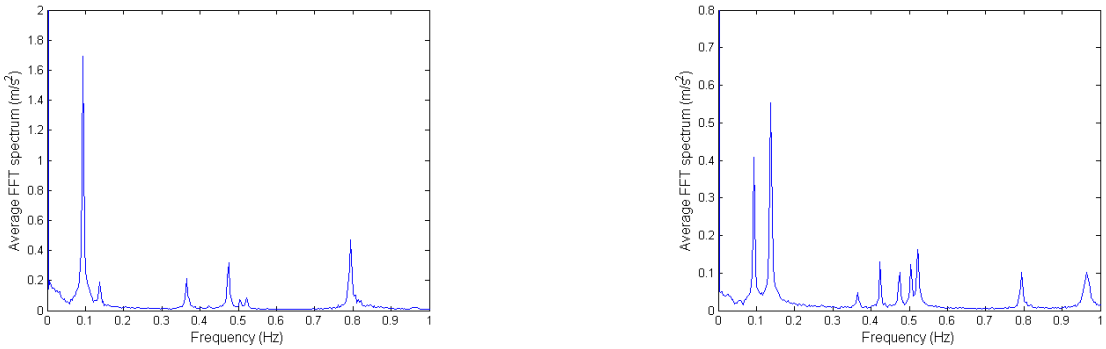

(c) Accelerometer: left – in short-axis direction; right – in long-axis direction

Fig. 18 Power spectra of the displacement/acceleration responses measured by the vision-based system, GPS and accelerometer

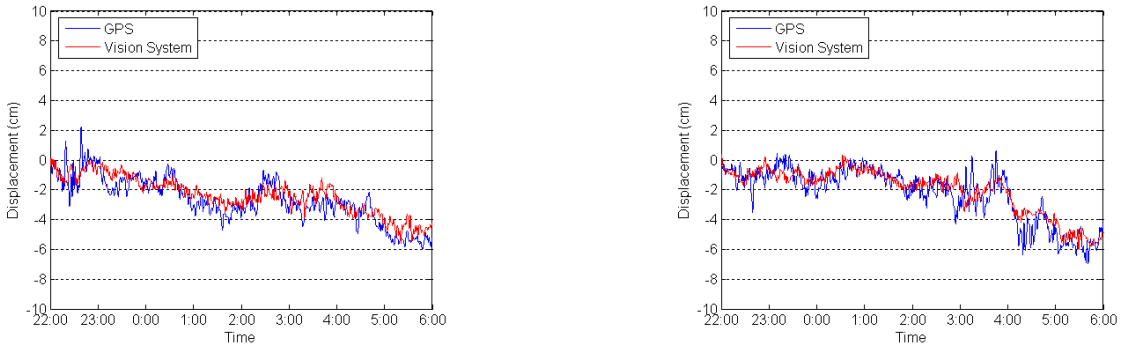

(a) Low frequency components (lower than 0.01 Hz): left – in short-axis direction; right – in long-axis direction

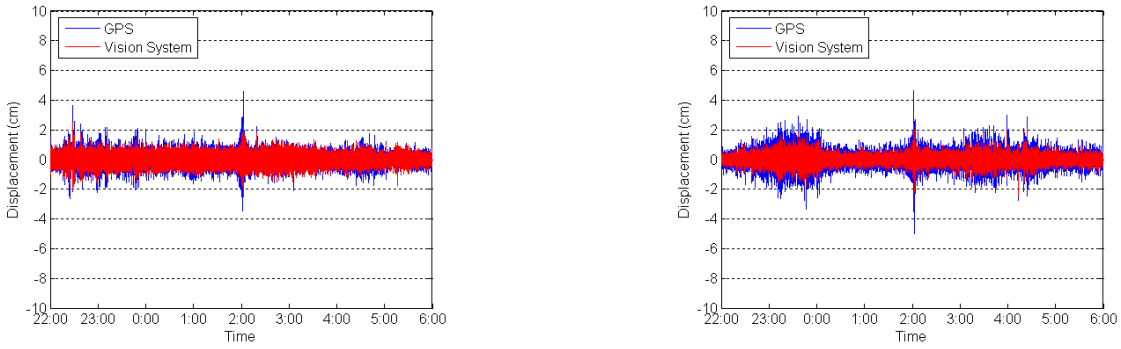

(b) High frequency components (higher than 0.01 Hz): left – in short-axis direction; right – in long-axis direction

Fig. 19 The separated low-frequency and high-frequency components of displacement responses

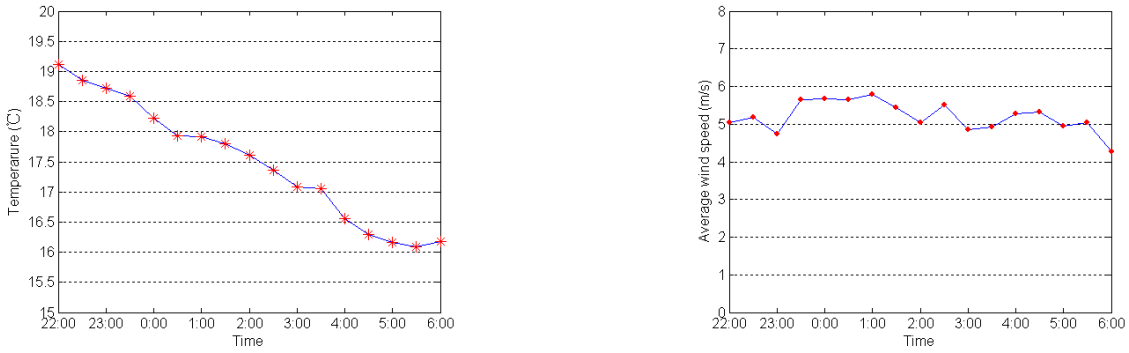

(a) Average temperature (b) Average wind speed

Fig. 20 The average temperature and wind speed at the top of main tower

Acknowledgements

The work described in this paper was supported by a grant from the Research Grants Council of the Hong Kong Special Administrative Region, China (Grant No. PolyU 152024/17E) and a grant from The Hong Kong Polytechnic University (Grant No. 1-ZVNF). The authors would also like to appreciate the funding support by the Innovation and Technology Commission of Hong Kong SAR Government to the Hong Kong Branch of Chinese National Rail Transit Electrification and Automation Engineering Technology Research Center (Grant No. K-BBY1).

References

Breuer, P., Chmielewski, T., Górski, P. and Konopka, E. (2002), "Application of GPS technology to measurements of displacements of high-rise structures due to weak winds", *J. Wind Eng. Ind. Aerod.*, **90**(3), 223-230. DOI: 10.1016/S0167-6105(01)00221-5.

Brownjohn, J., Rizos, C., Tan, G.H. and Pan, T.C. (2004), "Real-time long-term monitoring of static and dynamic displacements of an office tower, combining RTK GPS and accelerometer data", *P. Int. Symp. Eng. Sur. Constru. Works Struct. Eng.*, Nottingham, UK (CD-ROM).

Çelebi, M. (2000), "GPS in dynamic monitoring of long-period structures", *Soil Dyn. Earthq. Eng.*, **20**(5-8), 477-483. DOI:

10.1016/S0267-7261(00)00094-4.

Chan, T.H.T., Ashebo, D.B., Tam, H.Y., Yu, Y., Chan, T.F., Lee, P.C. and Gracia, E.P. (2009), "Vertical displacement measurements for bridges using optical fiber sensors and CCD cameras − a preliminary study", *Struct. Health Monit.*, **8**(3), 243-249. DOI: 10.1177%2F1475921708102108.

Fukuda, Y., Feng, M.Q. and Shinozuka, M. (2010), "Cost-effective vision-based system for monitoring dynamic response of civil engineering structures", *Struct. Control Health Monit.*, **17**(8), 918-936. DOI: 10.1002/stc.360.

Gordon, S.J. and Lichti, D.D. (2007), "Modeling of terrestrial laser scanner data for precise structural deformation measurement", *J. Surv. Eng.*, **133**(2), 72-80. DOI: 10.1061/(ASCE)0733-9453(2007)133:2(72).

Ji, Y.F. and Chang, C.C. (2008), "Nontarget image-based technique for small cable vibration measurement", *J. Bridge Eng.*, **13**(1), 34-42. DOI: 10.1061/(ASCE)1084-0702(2008)13:1(34).

Kijewski-Correa, T., Kareem, A. and Kochly, M. (2006), "Experimental verification and full-scale deployment of global positioning systems to monitor the dynamic response of tall buildings", *J. Bridge Eng.*, **132**(8), 1242-1253. DOI: 10.1061/(ASCE)0733-9445(2006)132:8(1242)

Lovse, J.W., Teskey, W.F., Lachapelle, G. and Cannon, M.E. (1995), "Dynamic deformation monitoring of tall structure using GPS technology", *J. Surv. Eng.*, **121**(1), 35-40. DOI: 10.1061/(ASCE)0733-9453(1995)121:1(35).

Li, X., Ge, L., Ambikairajah, E., Rizos, C., Tamura, Y. and Yoshida, A. (2006), "Full-scale structural monitoring using an integrated GPS and accelerometer system", *GPS Solut.*, **10**(4), 233-247. DOI: 10.1007/s10291-006-0023-y.

Lee, J.J., Fukuda, Y., Shinozuka, M., Cho, S. and Yun, C.B. (2007), "Development and application of a vision-based displacement measurement system for structural health monitoring of civil structures", *Smart. Struct. Syst.*, **3**(3), 373-384. https://doi.org/10.12989/sss.2007.3.3.373.

Nassif, H.H., Gindy, M. and Davis, J. (2005), "Comparison of laser Doppler vibrometer with contact sensors for monitoring bridge deflection and vibration", *NDT&E Int.*, **38**(3), 213-218. DOI: 10.1016/j.ndteint.2004.06.012.

Ni, Y.Q., Xia, Y., Liao, W.Y. and Ko, J.M. (2009), "Technology innovation in developing the structural health monitoring system for Guangzhou New TV Tower", *Struct. Control Health Monit.*, **16**(1), 73-98. DOI: 10.1002/stc.303.

Ni, Y.Q., Wong, K.Y. and Xia, Y. (2011), "Health checks through landmark bridges to sky-high structures", *Adv. Struct. Eng.*, **14**(1), 103-119. DOI: 10.1260/1369-4332.14.1.103.

Ni, Y.Q., Xia, Y., Lin, W., Chen, W.H. and Ko, J.M. (2012), "SHM benchmark for high-rise structures: a reduced-order finite element model and field measurement data", *Smart. Struct. Syst.*, **10**(4-5), 411-426. https://doi.org/10.12989/sss.2012.10.4_5.411.

Ni, Y.Q., Lin, K.C., Wu, L.J. and Wang, Y.W. (2017), "Visualized spatiotemporal data management system for lifecycle health monitoring of large-scale structures", *J. Aerosp. Eng.*, **30**(2), Paper No. B4016007. DOI: 10.1061/(ASCE)AS.1943-5525.0000622.

Olaszek, P. (1999), "Investigation of the dynamic characteristic of bridge structures using a computer vision method", *Measurement*, **25**(3), 227–236. DOI: 10.1016/S0263-2241(99)00006-8.

Ogaja, C., Wang, J. and Rizos, C. (2003), "Detection of wind-induced response by wavelet transformed GPS solutions", *J. Surv. Eng.*, **129**(3), 99-104. DOI: 10.1061/(ASCE)0733-9453(2003)129:3(99).

Park, H.S., Lee, H.M., Adeli, H. and Lee, I. (2007), "A new approach for health monitoring of structures: terrestrial laser scanning", *Comput. Aided Civil Infrastruct. Eng.*, **22**(1), 19-30. DOI: 10.1111/j.1467-8667.2006.00466.x.

Siringoringo, D.M. and Fujino, Y. (2006), "Experimental study of laser Doppler vibrometer and ambient vibration for vibration-based damage detection", *Eng. Struct.*, **28**(13), 1803-1815. DOI: 10.1016/j.engstruct.2006.03.006.

Seco, A., Tirapu, F., Ramírez, F., García, B. and Cabrejas, J. (2007), "Assessing building displacement with PGS", *Build. Environ.*, **42**(1), 393-399. DOI: 10.1016/j.buildenv.2005.07.027.

Siringoringo, D.M. and Fujino, Y. (2009), "Noncontact operational modal analysis of structural members by laser Doppler vibrometer", *Comput.Aided Civil Infrastruct. Eng.*, **24**(4), 1-17. DOI: 10.1111/j.1467-8667.2008.00585.x.

Tamura, Y., Matsui, M., Pagnini, L.C., Ishibashi, R. and Yoshida, A. (2002), "Measurement of wind-induced response of buildings using RTK-GPS", *J. Wind Eng. Ind. Aerod.*, **90**(12-15), 1783-1793. DOI: 10.1016/S0167-6105(02)00287-8.

Wahbeh, A.M., Caffrey, J.P. and Masr, S.F. (2003), "A vision-based approach for the direct measurement of displacements in vibrating systems", *Smart Mater. Struct.*, **12**(5), 785-794. DOI: 10.1088/0964-1726/12/5/016.

Xia, Y., Ni, Y.Q., Zhang, P, Liao, W.Y. and Ko, J.M. (2011), "Stress development of a super-tall structure during construction: field monitoring and numerical analysis", *Comput. Aided Civil Infrastruct. Eng.*, **26**(7), 542-559. DOI: 10.1111/j.1467-8667.2010.00714.x.

Ye, X.W., Ni, Y.Q., Wai, T.T., Wong, K.Y., Zhang, X.M. and Xu, F. (2013), "A vision-based system for dynamic displacement measurement of long-span bridges: algorithm and verification", *Smart. Struct. Syst.*, **12**(3-4), 363-379. https://doi.org/10.12989/sss.2013.12.3_4.363.

Ye, X.W., Yi, T.H., Dong, C.Z., Liu, T. and Bai, H. (2015a), "Multi-point displacement monitoring of bridges using a vision-based approach", *Wind Struct.*, **20**(2), 315-326. https://doi.org/10.12989/was.2015.20.2.315.

Ye, X.W., Yi, T.H., Wen, C. and Su, Y.H. (2015b), "Reliability-based assessment of steel bridge deck using a mesh-insensitive structural stress method", *Smart. Struct. Syst.*, **16**(2), 367-382. https://doi.org/10.12989/sss.2015.16.2.367.

Ye, X.W., Dong, C.Z. and Liu, T. (2016a), "Image-based structural dynamic displacement measurement using different multi-object tracking algorithms", *Smart. Struct. Syst.*, **17**(6), 935-956. https://doi.org/10.12989/sss.2016.17.6.935.

Ye, X.W., Dong, C.Z. and Liu, T. (2016b), "Force monitoring of steel cables using vision-based sensing technology: methodology and experimental verification", *Smart. Struct. Syst.*, **18**(3), 585-599. https://doi.org/10.12989/sss.2016.18.3.585.

Ye, X.W., Yi, T.H., Dong, C.Z. and Liu, T. (2016c), "Vision-based structural displacement measurement: system performance evaluation and influence factor analysis", *Measurement*, **88**, 372-384. DOI: 10.1016/j.measurement.2016.01.024.

Ye, X.W., Yi, T.H., Su, Y.H., Liu, T. and Chen, B. (2017), "Strain-based structural condition assessment of an instrumented arch bridge using FBG monitoring data", *Smart. Struct. Syst.*, **20**(2), 139-150. https://doi.org/10.3390/s18020491.